Modeling of hydrogen trapping in the deformed Pd and Pd$_{77}$Ag$_{23}$ alloy

Y. Cao [a,*], H.L. Li [a], J.A. Szpunar [a], W. Shmayda [b]

[a] *Department of Metals and Materials Engineering, McGill University, Montreal, PQ, Canada H3A 2B2*
[b] *Lab for Laser Energetics, University of Rochester, Rochester, NY 14623-1299, USA*

Abstract

The effects of Pd and Pd$_{77}$Ag$_{23}$ alloy membrane microstructures on hydrogen permeation have been investigated using the electrochemical permeation method. Deformation and annealing have been used to modify the membrane microstructures. The delay of hydrogen permeation in palladium increases when the degree of deformation is increases. The annealing of deformed palladium and Pd$_{77}$Ag$_{23}$ accelerates hydrogen diffusion. The annealed metals release hydrogen more rapidly than deformed metals. Also, the Pd$_{77}$Ag$_{23}$ alloy needs more time to release hydrogen than pure palladium. The solubility of hydrogen increases in both palladium and Pd$_{77}$Ag$_{23}$ when the amount of deformation is increased. A hydrogen trapping model was developed, which allows the prediction of trends of hydrogen permeation through membranes having different structures.
© 2004 Elsevier B.V. All rights reserved.

Keywords: Hydrogen Permeation; Modeling; Pd$_{77}$Ag$_{23}$ alloys; Palladium; Trapping; Deformation

1. Introduction

Membranes are widely used to extract or separate hydrogen from other gases. Membranes of palladium and Pd–Ag alloys have been applied in many reactors due to their high hydrogen permeability. Palladium and Pd–Ag alloys are easily formed into tubes that are used to fabricate hydrogen extraction units [1–3]. The cold rolled sheets of palladium and palladium–silver alloys are also used in the chemical and energy industries [3]. Cold rolling will produce microstructural defects, such as dislocations. Defects will interact with hydrogen when these materials are used in a hydrogen environment. The trapping of hydrogen by defects influences hydrogen transport properties. There are two models used to explain the trapping phenomenon [4,5]. One is based on the assumption of equilibrium between trapping sites and normal lattice sites; another one is based on the rates of hydrogen trapping and escaping from the trap. In previous research, almost all attempts to explain hydrogen trapping were based on continuum diffusion approximations by solving the diffusion equations with some special boundary conditions [4,5]. Such an approach may not lead to adequate approximations for trapping on the atomic scale [6].

The present work focuses on experimental investigations into the effect of trapping on hydrogen permeation in palladium and Pd–Ag alloys. A model to simulate this phenomenon has been proposed to explain experimental results.

2. Experimental

The materials used in this study are Pd and Pd$_{77}$Ag$_{23}$ alloy membranes. The Pd$_{77}$Ag$_{23}$ alloys foils were subjected to 80% cold rolling and had a thickness of 127 μm. Palladium thickness is 105 μm with 20, 50, and 82% cold rolling. Pd and Pd$_{77}$Ag$_{23}$ alloys are annealed, respectively, at 250 °C for 3 h and 550, 700, 850 °C for 1.5 h. Orientation imaging microscopy (OIM) installed on Philips XL-30 SEM with TSL orientation imaging system was used to observe the microstructure of deformed palladium. To prepare samples, mounting with carbon powder and hot pressing at 250 °C was used. The microstructure is normally difficult to observe using optical and scanning electron microscopes. The microstructure of the deformed samples was also observed using the Philips TM transmission electron microscope (TEM). The dislocation density in deformed Pd and Pd–Ag alloy

* Corresponding author. Present address: Department of Metallurgy and Materials Engineering, University of Connecticut, 97 N. Eagleville Road, Storrs, CT 06269, USA.

E-mail address: ericcao@mail.ims.uconn.edu (Y. Cao).

membranes was calculated from analysis of broadening of X-ray diffraction lines [7,8].

The electrochemical technique for hydrogen permeation has been used. The double cell apparatus has been described previously [9,10]. Before permeation, the experimental sample was washed and dried, and placed between cells. The hydrogen permeation tests were performed in a 0.1N NaOH solution with a cathodic current of $0.1\,\mathrm{mA\,cm^{-2}}$. The hydrogen permeation current through the membrane was measured and recorded. The diffusion coefficient D is calculated by time lag method. The steady-state flux of hydrogen through the foil is directly proportional to the diffusion coefficient. With Faraday's and Fick's First Law in steady-state permeation experiments [10,11], one can obtain

$$C_0 = \frac{I_{ss}L}{FD} \tag{1}$$

where C_0 is the concentration of absorbed hydrogen at the input surface that corresponds to a certain charging current and I_{ss} is steady-state permeation current density. L is the sample thickness and F is Faraday constant.

3. Results

3.1. Microstructure in Pd and Pd–Ag membranes

The microstructure of palladium after 850 °C annealing was analyzed using optical microscopy. The grain size of palladium is around 20 μm. The microstructure of deformed palladium is shown in Fig. 1. Fig. 1 was obtained from an orientation imaging microscopy image, which uses color to distinguish different orientation of grains. From Fig. 1, one can see that elongated grains are arranged along the rolling direction. The average grain size of palladium is 15 μm. It is very important to know the grain size of palladium to determine hydrogen permeation behavior. A transmission electron microscope image of 82% deformed palladium is shown in Fig. 2. Heavy cold rolling creates a more heterogeneous or cellular arrangement of dislocations. High-density of dislocations with cellular substructure have been observed. The
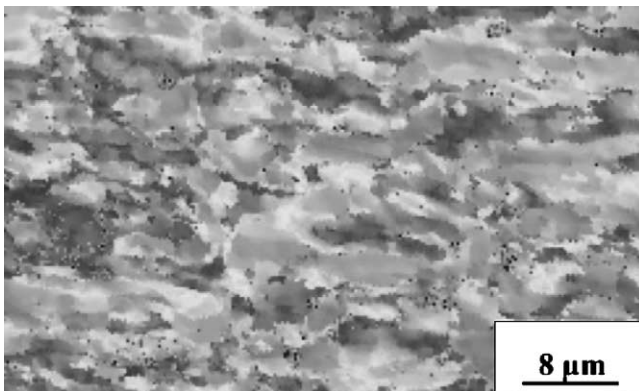

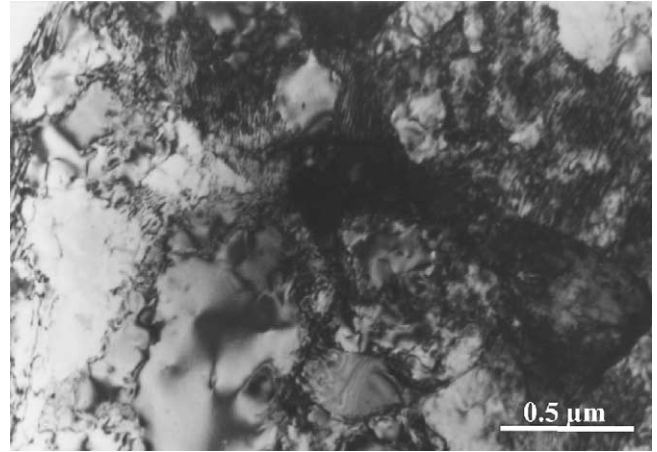Fig. 1. OIM microstructure of deformed palladium.

Fig. 2. TEM image of dislocation substructure of deformed Pd.

cellular substructure includes walls with a high dislocation density surrounding regions with a low dislocation density. A cellular dislocation substructure is produced by deformation and recovery of metals with high stacking fault energy at a large strain. Palladium has high stacking fault energy and the amount deformation (82%) in this Pd sample was high, so a microstructure with high dislocation density was formed.

To measure dislocation density in deformed palladium, the diffraction broadening method was used [7,8]. X-ray diffraction line profiles analysis was used to estimate dislocation densities of Pd and $Pd_{77}Ag_{23}$ alloy as shown in Table 1. From Table 1, it can be seen that the deformed samples have much higher dislocation density than the annealed ones. These dislocations make hydrogen transport and hydrogen discharge from the specimen more difficult.

3.2. Effect of deformation of Pd and $Pd_{77}Ag_{23}$ alloy on hydrogen permeation

3.2.1. Effects of cold rolling on hydrogen permeation

The permeation transients of cold rolled and annealed $Pd_{77}Ag_{23}$ alloy are plotted in Fig. 3. The anodic current density increases smoothly with increasing charging time

Table 1
Dislocation densities in Pd and Pd $_{77}Ag_{23}$ alloys

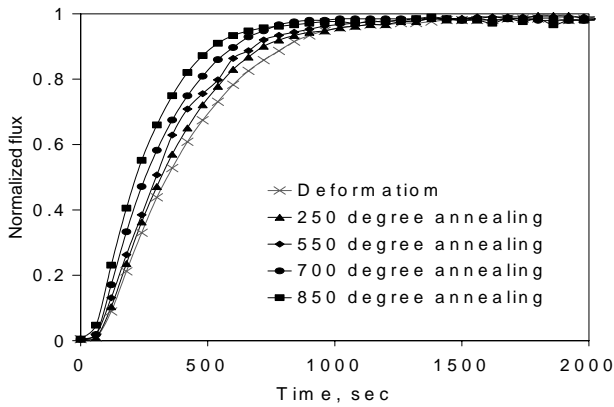| Materials	Dislocation density, $(\times 10^{12}\,\mathrm{cm^{-2}})$
Pd	
850 °C, 1.5 h	0.07
Deformation 20%	0.38
Deformation 50%	1.7
Deformation 82%	2.9
$Pd_{77}Ag_{23}$	
Deformation	3.4
250 °C, 3 h	2.1
850 °C, 1 h	0.9

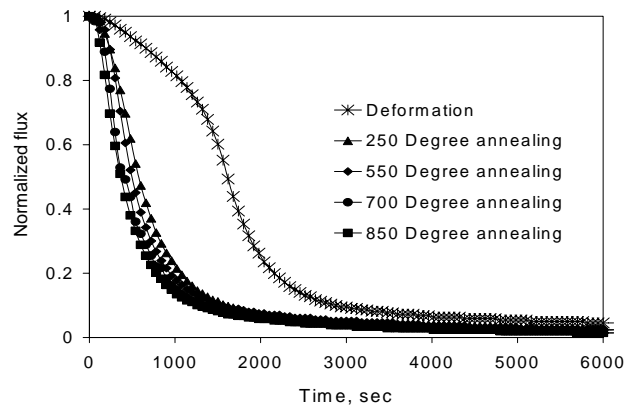Fig. 3. Hydrogen permeation transients for $Pd_{77}Ag_{23}$ membranes.

Fig. 5. Hydrogen decay for $Pd_{77}Ag_{23}$ membranes.

and finally tends towards a constant. The permeation current of deformed samples increased more slowly than the annealed sample with the same thickness because of higher probabilities of hydrogen trapping in deformed samples. It can be concluded that deformation produces an imperfect structure with dislocations and point defects, which serve as hydrogen trap sites. In the $Pd_{77}Ag_{23}$ alloy annealed at 250 and 550 °C, the permeation current increases faster. The reason for this increase is that low temperature annealing leads to recovery and reduces residual stress in the sample, this permits hydrogen to diffuse more easily than in the deformed state. The increase of the permeation current in the $Pd_{77}Ag_{23}$ alloy annealed at 850 °C is the fastest among the specimens annealed at five different conditions. The annealing temperature (700 and 850 °C) was above the recrystallization temperature of the $Pd_{77}Ag_{23}$ alloy and thus diminishes the number of imperfections. The $Pd_{77}Ag_{23}$ alloy that has fewer numbers of defects in the structure has higher hydrogen diffusion. The permeation transients of cold worked and annealed palladium are plotted in Fig. 4. The trend here is similar to that observed in the palladium alloy. At low deformation (20%), there are some small differences. When deformation increased to 50%, the permeation is evidently delayed. At 82% deformation, the permeation is still delayed

but the changes are not so dramatic. This behavior shows that hydrogen occupies sites of low energy (deep traps) first and after saturation of these sites, hydrogen occupies the remaining sites as in well-annealed palladium specimens.

The hydrogen decay curves for $Pd_{77}Ag_{23}$ alloy and palladium membranes are shown in the Figs. 5 and 6, respectively. For the annealed palladium, the hydrogen permeation current decreases faster than for the deformed one. The hydrogen diffusivity depends on the trap density, trap strength, degree of saturation of traps, and reversibility of trapping. After saturation of traps in palladium and its alloys, the hydrogen in palladium will diffuse through normal sites. For the defect trap sites, hydrogen has to overcome additional energy to jump out. The process is more difficult and the residence time of hydrogen in the trap sites is longer. The permeation in deformed $Pd_{77}Ag_{23}$ decays more slowly than in pure palladium. It is known that the lattice parameter of the $Pd_{77}Ag_{23}$ alloy has a higher value than that of pure palladium. So the palladium lattice expansion in the $Pd_{77}Ag_{23}$ alloy structure produces a lattice micro-strain [12]. Thus both the specimen deformation and the presence of the silver element may be a reason for a higher probability of hydrogen trapping in $Pd_{77}Ag_{23}$ alloy and therefore low rate of hydrogen de-trapping. Fig. 5 illustrates differences between the hydrogen decay in various investigated specimens.
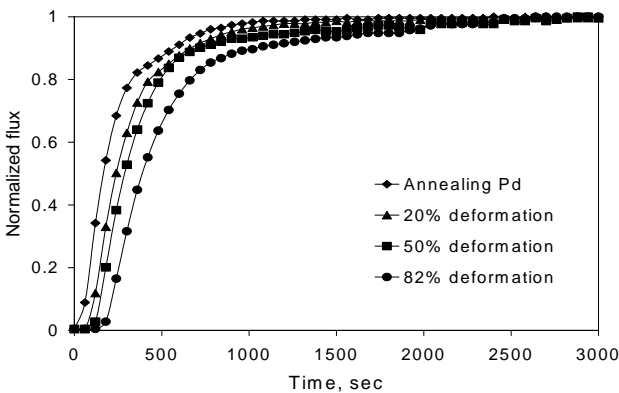

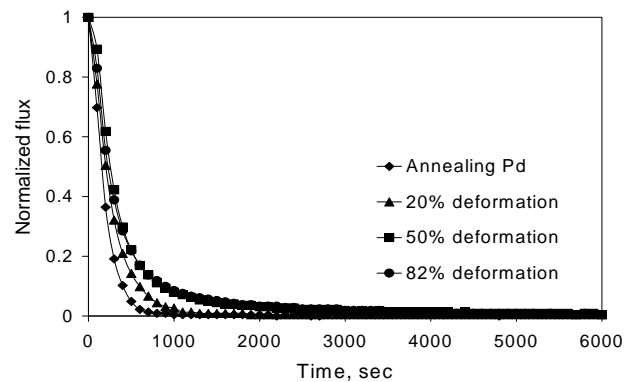Fig. 4. Hydrogen permeation transients for palladium membranes.

Fig. 6. Hydrogen decay permeation for palladium membranes.

Table 2
Hydrogen diffusion and trapping parameters of palladium and Pd$_{77}$Ag$_{23}$ alloys

Materials	Apparent diffusion coefficient, D ($\times 10^{-7}$ cm^2 s^{-1})	C_0 ($\times 10^{-5}$ mol cm^{-3})	Trap density, N_T ($\times 10^{17}$ cm^{-3})
Pd			
850 °C, 1.5 h	2.6	4.5	4.0
Deformation			
20%	2.4	5.5	7.1
50%	1.7	6.8	23.7
82%	1.6	7.5	24.1
Pd$_{77}$Ag$_{23}$			
Deformation	2.0	7.1	14.4
250 °C, 3 h	2.2	6.1	9.5
550 °C, 1.5 h	2.4	5.8	6.9
700 °C, 1.5 h	2.7	5.2	3.0
850 °C, 1.5 h	2.9	4.5	0.12

The concentration of absorbed hydrogen (C_0) at the input side is presented in Table 2. The hydrogen concentration decreased after annealing of deformed palladium and Pd$_{77}$Ag$_{23}$ alloy. This means that cold working increases the solubility of hydrogen in palladium due to the interaction of dissolved hydrogen atoms with the stress field and dislocations [13].

3.2.2. Hydrogen trapping analysis for metals with defects

When a metal membrane has been charged with hydrogen, hydrogen will absorb into the membrane surface and diffuse through it, then it will exit from the membrane by desorption from the opposite side. Usually, diffusion of hydrogen in the membrane is the slowest step in the overall hydrogen permeation process. If there are defects such as dislocations, grain boundaries, non-metallic inclusions, and other internal interfaces in this membrane, hydrogen will be trapped in defects. The TEM results show that deformed samples have a lot of dislocations. Normally, dislocations are the most common hydrogen traps in metals.

Octahedral sites in FCC palladium form an FCC lattice with the same lattice constant as the host lattice. The interstitial lattice is displaced with respect to the host lattice. There is one octahedral site per host atom. Neutron scattering and channeling experiments have shown that hydrogen in palladium occupies the octahedral sites [14]. The density of interstitial octahedral sites per unit volume, N_L, is calculated based on the number of interstitial octahedral sites per unit cell and metals lattice parameters. In the near saturation limit where there is no full occupancy for the reversible traps, the trap densities can be calculated [4]. It can be found that if the trap density increases, the diffusion coefficient is lowered. The trap density decreases after annealing of palladium and Pd$_{77}$Ag$_{23}$. When annealed at 250 °C, the trap density is reduced by about 50%. For a Pd$_{77}$Ag$_{23}$ alloy well annealed at 850 °C, the trap density is reduced by two orders of magnitude. The trap density of palladium annealed at 850 °C also decreases to nearly half of the density in 20%

deformed palladium. This confirms that annealing can significantly decrease trapping of hydrogen for palladium and Pd$_{77}$Ag$_{23}$ alloys [15].

4. Permeation model and computer simulation

4.1. Trap mechanism analysis and trapping maps

When a metal membrane has been charged with hydrogen, hydrogen will be absorbed into the membrane and diffuse through it. If there are defects in this membrane, hydrogen will be trapped in defects. From our results, it was concluded that deformation produces a high-density of dislocations, which normally serve as hydrogen traps. A transmission electron microscope image of 82% deformed palladium after hydrogen charging is shown in Fig. 7. High-density dislocations still exist in palladium. Some dislocation sites may serve as traps for hydrogen atoms. There is evidence that hydrogen can be trapped by dislocations [16,17]. Because the volume of atoms at grain boundaries in Pd is very low (<1%), the trapping effects of grain boundaries are less important than that of dislocations. Therefore, it is reasonable to disregard the effect of grain boundaries or count the trapping in grain boundaries as a part of dislocations trapping. As a result, the defects responsible for trapping are dislocations. To simulate hydrogen trapping, we consider two kinds of lattice sites (normal and defect sites), these two classes have different hydrogen residence time (Fig. 8). The majority of
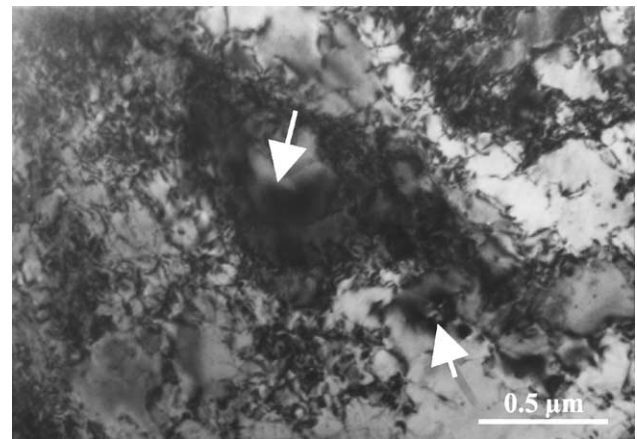

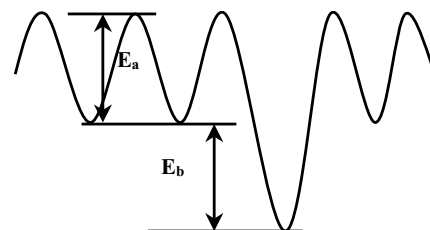Fig. 7. TEM microstructure of Pd after hydrogen charging.

Fig. 8. Energetic schematic of hydrogen diffusion with trapping sites.

sites available for occupancy by hydrogen atoms are normal lattice sites having activation energy of diffusion, E_a. The remaining sites are defects acting as trapping sites, which have additional trap binding energy, E_b. The total energy needed for a hydrogen atom to jump out off a trap site is $E_a + E_b$, which represents a high-energy barrier for hydrogen escape. Hydrogen trapping phenomenon is due to attractive interaction between the dissolved hydrogen atoms and defects. The main deformation defects are dislocations because palladium is a single phase and the dislocation density after deformation is very high, which has been illustrated by TEM results for palladium (Fig. 2). The random walk method has been used to deal with the effects of trapping on hydrogen diffusion. Diffusivity is calculated based on the time and average distance that a group of hydrogen atoms have migrated from their initial sites. As it was already mentioned, lattice sites in the sample are divided into normal and trap sites. Following this assumption, a computer sample with dislocation defects distributed randomly is generated according to the estimated volume of trap sites. The cross-section of the computer sample representing the distribution of dislocations will be called a trapping map (Fig. 9). In the trapping map, number 1 represents defect sites and number 0 represents normal sites.

4.2. The model description of hydrogen trapping

For most of the permeation experiments, hydrogen has been charged in the direction perpendicular to the membrane plane. According to recommendations by Hutchings et al. [18], the metal membranes specimens must have a ratio larger than 1:10 of the specimen thickness to the diameter of charging area, to have reliable hydrogen permeation measurements. Actually, our experiments used 1:40 to 1:200 ratios. This means that hydrogen diffusion is mainly through the direction perpendicular to the membrane. The random walk method has been used to evaluate hydrogen diffusion [19]. By checking the passing and residence time in the sample for individual hydrogen atoms, statistical total hydrogen flux can be calculated and has been compared to real experimental data. To introduce dislocation defects, the computer simulation sample has two dimensions, which are the same as the cross-sections of metal membrane samples. In the computer sample, the length and the width correspond to the permeation area size and the thickness of a metal membrane respectively. The size of the computer simulation sample was set to a length of 100 units and a width of 10 units with 10:1 ratio, which is same as the ratio of the diameter of permeation area to the thickness of the metal membrane sample. Actually, the length of the computer simulation sample can be 1000 units or more, as long as the ratio of the length to the width of the computer sample is larger than 10:1. In order to simplify the situation, dislocations are presented in vertical or horizontal lines connecting defect sites with random lengths between 1 and 10 units. The dislocation or grain boundary traps will become saturated when certain amounts of hydrogen are captured in the traps [20]. After traps are saturated with hydrogen atoms, other hydrogen atoms can diffuse through the trapping sites. We assume that the trapping site will become saturated after only one hydrogen atom occupies the site, which means only one hydrogen atom resides in one trapping site at one time. In reality, a trapping site may hold more than one hydrogen atom to become saturated. However, this assumption makes no difference because the simulation is qualitative. The shape of the permeation curve is the same no matter how many hydrogen atoms saturated the trapping site.

4.3. Simulation details and process of hydrogen permeation

The main idea of the present trapping model has been discussed and trap maps have been produced. Now, it is necessary to introduce more details to be able to run this simulation. Five conditions should be clarified to build the simulation model of hydrogen permeation.

1. Before charging with hydrogen, there is almost no hydrogen in the metal membranes. This is a normal case because residual hydrogen in the membrane has been extracted by holding a constant anodic potential at the exit side for a long time. The extraction of hydrogen is a standard procedure for electrochemical permeation. The boundary condition for hydrogen permeation assumes a constant hydrogen pressure on the entry side. When the thickness of the Pd membrane is over $50\,\mu m$, there is less than 100% of the charged hydrogen appearing on the exit side [21]. Even through a palladium membrane has

```
1110000000010111111111110100000010000000001010000000001001010100001000100000000010100111111100111111
0000000000000011001101011010000000000000001011000000001111111100010000100000000000000000110000111110
0000000011110001001100110010111111111110000111111000000100000000011111110100011111000000000001111111
0100000000000110011010101111110000100000010011100000010010001011100000001000000001111110000110000111110
1111100001100111111111001010000100000010011000110000001010100000100001111111000000000001101001101010
0010000001101101001111111000100001000000010011100000000001111111000100001111000000100010010010011110
1111110001110110011010100101000010000000010011100000000001111010001000000000000001000100100100010111
0110000101110110111000110101000010000000011000000000001110101000000000000010001000100100100010110
1111111111111111110101101000000100000000011100111111111101010001111100011111111100100100000110111
0001111111111101110101111011111000000000101000000000110111111111000110000000011111111010100000111110
```
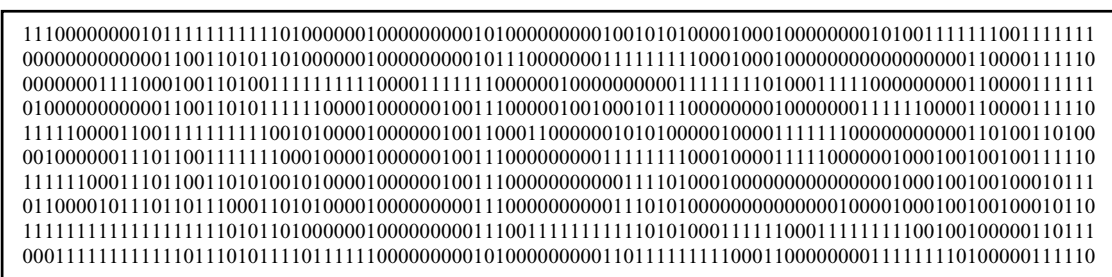
Fig. 9. Schematics of hydrogen trapping map in the metal membrane.

been charged galvanostatically, it still can hold enough hydrogen on the entry side for hydrogen permeation to take place. The hydrogen concentration at the exit side is always zero for permeation since the exit side is held potentiostatically at a sufficient potential to ensure that all hydrogen from the membrane interior is instantly oxidized [9,22,23].

2. As it was mentioned before, the volume fraction of grain boundaries in polycrystalline Pd is very low (<1%) and the trapping effects of grain boundaries are not as pronounced as trapping at dislocations. In this case only lattice diffusion is dealt with. The main attention focuses on hydrogen trapping at dislocations in a metal membrane.

3. There exists the equilibrium between hydrogen atoms at trapping sites and normal lattice sites [4]. Sometimes, the thermal energy is large enough for the hydrogen atoms to jump out of the trap sites. The probability of hydrogen escaping a trapping site is calculated from $\exp(-E_b/kT)$. E_b is the binding energy, which represents the barrier level and depends on the type of defects. After jumping out from trapping potential well, the hydrogen atom will diffuse normally. The trap site is saturated after one hydrogen atom fills this site. When one hydrogen atom occupies a site, this site is now considered as a non-trapping site for hydrogen. This means that trapping effects will diminish in the sample.

4. The simulation run 20 loops at the plateau region for hydrogen permeation flux, to make sure that the permeation curves really reached steady-state. Then the simulation starts the desorption process, which is the hydrogen releasing process. When a permeation flux is reduced to 1% of the steady-state value, the whole simulation process stops. Although the criteria is set up as 1%, it can be changed to 2 or 3%, which will generate similar results.

5. The random walk process has been used to simulate hydrogen diffusion through membranes. The flux is calculated by counting the number of hydrogen atoms exiting the membrane in a given interval of simulation time at the exit side with a certain amount of hydrogen charged at the entry side. By plotting flux vs. simulation time, permeation curves have been obtained.

The diagram illustrating the simulation process is shown in Fig. 10. Accordingly, there are seven steps to simulate the trapping process. (1) Input parameters: this includes filename, percent volume of trapping sites, binding energy, E_b, and the temperature in Kelvin. (2). Produce trap map: this produces dislocations with vertical or horizontal lines with random lengths between 1 and 10 units. (3) Hydrogen diffusion with trapping: this traces hydrogen atoms diffusion in metals with trapping sites. (4) Flux calculation: this counts the amount of hydrogen atoms passing through the membrane at a given time interval and compares the flux with the previous time. (5) Charging hydrogen stops and desorption process starts: this stops hydrogen supply and starts the decay process when a constant flux plateau has been reached
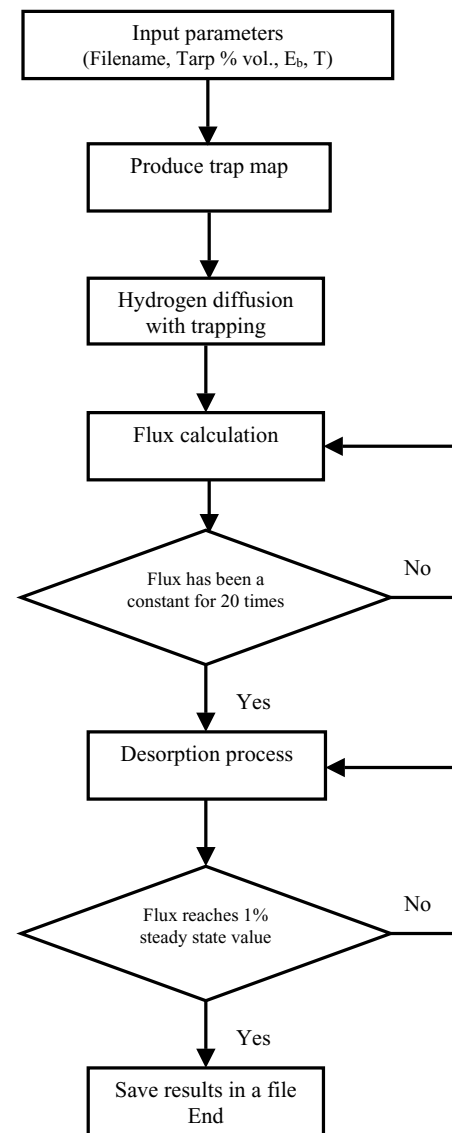

Fig. 10. Procedure of hydrogen diffusion simulation.

and the flux does not change much for 20 times. (6) Stop desorption process: this stops desorption and starts saving files when the flux reaches 1% of steady-state flux value. (7) Save a file and end the processing: this will save calculation results in a file named by the user and end the whole program.

4.4. Comparison of hydrogen trapping behaviors with the model prediction

In order to calculate the transient hydrogen permeation curve, the binding energy (E_b) should be determined. The binding energy is related to the character of materials and the kind of defects in the membranes. Here 0.1 eV has been chosen as E_b for palladium with dislocations as defects, which is a normal case for FCC metals [24]. By changing the trapping volume, different hydrogen permeation curves
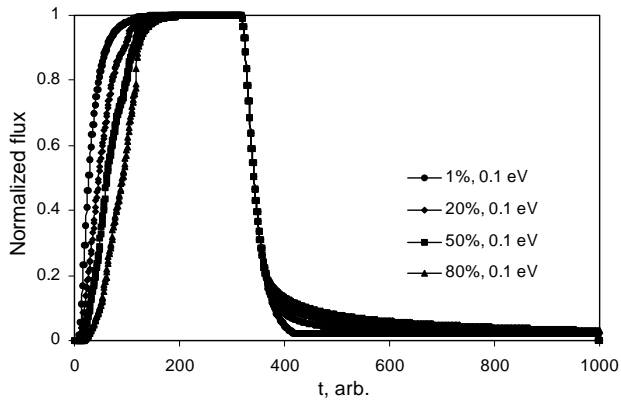
Fig. 11. Simulation of hydrogen flux of metal membranes with different volumes of trapping sites.

Fig. 13. Comparison of simulation with experiment data for Pd hydrogen permeation.

have been obtained. With the same kind of defects (same binding energy), hydrogen permeation processes have been delayed when trapping volume increased. Also, hydrogen decay curves have similar trends of change as the experimental data. Increasing trapping volume has retarded hydrogen release from the exit side. When comparing the present results of simulation (Fig. 11) with the experiments (Figs. 3–6), it can be seen that they correspond with each other. When the percent of deformation increases to produce more dislocations, the trapping volume increases and this causes a hydrogen permeation delay, because the trapping sites hold hydrogen for a longer time than the normal sites. Both experimental hydrogen permeation and hydrogen decay curves show the same trends when trapping sites increase as the simulation presented. This validates the model for hydrogen permeation with trapping. Furthermore, using this model one can evaluate the effect of binding energy on hydrogen permeation (Fig. 12). From Fig. 12, it can be seen that higher binding energy delays hydrogen permeation and decay. The time-lags obtained from the model and the experiments are in a linear relationship (Fig. 13). One can change three parameters in the model: binding energy, temperature, and trapping volume at the same time. This is one of the
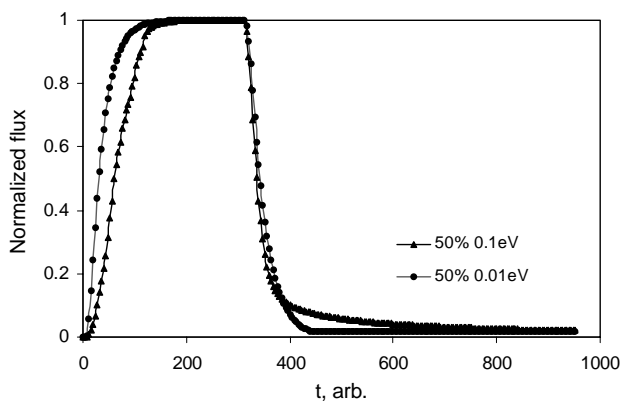
many advantages in using this computer model for the estimation of hydrogen permeation and transport. When bulk data are available, different parameters of the model can be obtained. The calculation time of a permeation curve is less than 10 s in a 500 MHz PC computer. If a sample has an initial hydrogen concentration before charging, the model can still be used for the simulation of hydrogen permeation by adjusting the trapping volume. Of course, one should know the former charging condition and the amount of hydrogen in the sample in order to get a volume of trapping sites.

5. Conclusions

1. The study of hydrogen permeation in deformed palladium and $Pd_{77}Ag_{23}$ has shown that hydrogen permeation has been delayed because hydrogen trap sites have been introduced by deformation. When increasing the amount of deformation in palladium, hydrogen permeation in palladium is delayed even more. The annealing of deformed palladium and $Pd_{77}Ag_{23}$ at 250 °C reduces the number of trap sites, so permeation is faster than in the deformed metals. The annealing of deformed palladium and $Pd_{77}Ag_{23}$ at 850 °C makes hydrogen diffusion even faster. Recrystallization annealing reduces the number of trap sites and allows recovery of the hydrogen permeation characteristics in palladium and palladium alloys.
2. After deformation and annealing, palladium and $Pd_{77}Ag_{23}$ have different hydrogen decay characteristics. The annealed metals release hydrogen more rapidly than the deformed metals. The $Pd_{77}Ag_{23}$ alloy needs more time to release hydrogen because of combining effects of deformation and the lattice distortion. The solubility in deformed palladium and $Pd_{77}Ag_{23}$ is increased by deformation.
3. Hydrogen has been trapped at dislocations in the specimens deformed to different reductions in thickness. Because hydrogen residence time at trap sites is longer than at normal sites the hydrogen diffusion has been delayed.

Fig. 12. Simulation results for metal membranes with two different binding energy values.

Time lag measurements of deformed palladium and its alloys established that the traps induced by deformation could be saturated. The trap densities in palladium rapidly increase from 20 to 50% in deformed specimens, and then increase rather slowly. The dislocations and local residual stress introduced by deformation are thought to be trapping sites for hydrogen.

4. A hydrogen trapping model has been developed to simulate trapping mechanisms and diffusion. The experimental data are in good qualitative agreement with the model. The model can generate random trapping site distributions and diffusion profiles. The simulation clearly generates results very quickly compared to experiments. The model can explain the effects of trapping on hydrogen permeation through thin membranes. If a sample has an initial hydrogen concentration before charging, the trapping volume has to be adjusted accordingly. One should know the former charging conditions and the amount of hydrogen in the sample in order to get the correct trapping volume.

Acknowledgements

References

[1] S. Tosti, L. Bettinali, V. Violante, Int. J. Hydrogen Energy 25 (2000) 319.
[2] J. Park, T. Bennett, J. Schwararzmann, S. Cohen, J. Nucl. Mater. 220–222 (1995) 827.
[3] F. Lewis, Int. J. Hydrogen Energy 216 (1996) 461.
[4] R. Oriani, Acta Metall. 18 (1970) 147.
[5] A. McNabb, P. Foster, Trans. TMS-AIME 227 (1963) 618.
[6] C. Flynn, Phys. Rev. 133 (1964) A587.
[7] F. Williamson, R. Smallman, Philos. Mag. 1 (1956) 34.
[8] L. Revay, Electrodeposition Surf. Treat. 3 (1975) 139.
[9] N. Boes, H. Zuchner, J. Less Met. 49 (1976) 223.
[10] M. Devanathan, Z. Stachuski, Proc. R. Soc. 270A (1962) 90.
[11] J. Early, Acta Metall. 26 (1997) 1215.
[12] Y. Sakamoto, S. Hirata, H. Nishikawa, J. Less-Common Met. 88 (1982) 387.
[13] T. Flanagan, J. Lynch, J. Less-Common Met. 49 (1976) 25.
[14] P. Dederichs, K. Schroeder, R. Zeller, Point Defects in Metals II, Sringer-Verlag, New York, 1980, p. 177.
[15] Y. Cao, J. Szpunar, W. Shmayda, Defect Diffusion Forum 194–199 (2001) 1081.
[16] A. Brass, J. Chene, Mater. Sci. Eng. A242 (1998) 210.
[17] B. Heuser, J. King, Metall. Trans. 29A (1998) 1593.
[18] R. Hutchings, D. Ferriss, A. Turnbull, Br. Corros. J. 28 (1993) 309.
[19] P. Shewmon, Diffusion in Solids, second ed., TMS, 1989, p. 61.
[20] C. Wert, Ann. Res. Mater. Sci. 13 (1983) 139.
[21] S. Schuldiner, J. Hoare, J. Electrochem. Soc. 103 (1956) 178.
[22] A. Atrens, D. Mezzanotte, N. Fiore, M. Genshaw, Corros. Sci. 20 (1980) 673.
[23] H. Tsubakino, R. Nishimura, Corros. Eng. 49 (2000) 261.
[24] G. Young, J. Scully, Acta Mater. 46 (1998) 6337.